

Natural patterning of templates on GaAs by formation of cracks

Yuxin Song,¹ Hao Xu,¹ Yaoyao Li,^{1,a} Mahdad Sadeghi,²
and Shumin Wang^{1,2,a}

¹State Key Laboratory of Functional Materials for Informatics, Shanghai Institute of Microsystem and Information Technology, Chinese Academy of Sciences, 200050, Shanghai, China

²Department of Microtechnology and Nanoscience, Chalmers University of Technology, 41296, Gothenburg, Sweden

(Received 29 March 2015; accepted 11 June 2015; published online 22 June 2015)

Substrate pre-patterning is an effective way to overcome large lattice mismatch and suppress threading defects in the growth of heterostructures. In this work, a new concept was proposed to form natural patterns on commercial substrates monolithically by the formation of surface cracks. Tensile strain was intentionally brought in with a GaAs or GaNAs layer above an InGaAs layer on GaAs substrates. Surface crack patterns successfully formed during the strain relaxation. The strain in a 1 μm buffer layer atop the pattern was found effectively relaxed. Detailed residual strain distribution was simulated by the finite element method. © 2015 Author(s). All article content, except where otherwise noted, is licensed under a Creative Commons Attribution 3.0 Unported License. [<http://dx.doi.org/10.1063/1.4922961>]

Lattice as well as thermal expansion mismatch has always been an issue for the design and growth of semiconductor heterostructures and devices. In order to maintain pseudomorphic growth during epitaxy without strain relaxation, which will lead to generation of dislocations and surface roughness, only materials closely lattice matched to the well-established commercial substrates, such as GaAs or InP, can be selected. With the aim of breaking this limitation, metamorphic growth is one of the most studied approaches to produce a relaxed buffer layer with a different lattice constant compared with the substrate. Among many different methods of metamorphic growth, the graded buffer layer is one of the most successful ones leading to low threading dislocation (TD) density and relatively smooth surface.^{1–4} This gives the advantage of using large, low-cost substrates, while still making it possible to produce devices with more optimized structure. The success of the metamorphic method has resulted in commercial electronic devices, such as high-electron mobility transistors (HEMTs) on GaAs,^{5,6} and large progress of GaAs based telecom lasers to improve the temperature stability.^{7–9} HEMTs are small area devices which can tolerate relative high TD density. However, for optoelectronic devices like lasers it is much more challenging, hindering the commercialization process. Several TD blocking methods were implemented to further reduce the TD density, e.g. quantum dot layers,¹⁰ superlattices,¹¹ and dilute nitrides layers with lattice hardening effects.^{12,13} Further improvement of the quality of metamorphic buffer layers is desired for high performance metamorphic optoelectronic devices.

Recently, the technique of pre-patterning the substrates has shown very promising results. The patterns with limited sizes allow for the strain to relieve partly through elastic deformation and the TDs generated by plastic deformation can easily glide to the edges of the patterns and terminate. High quality Ge and GaAs templates have been produced with this method on silicon substrates.¹⁴ However, the pre-patterning process may introduce unintended contamination and increase process complexity and production costs. In this work, we propose and explore a new concept to form natural patterns on commercial substrates monolithically by the formation of surface cracks. Tensile

^aE-mail: yyli@mail.sim.ac.cn, shumin@chalmers.se



TABLE I. The structures of the crack forming layers of the samples.

Sample No.	Crack forming layers
A1	200 nm GaAs
B1	100 nm GaN _{0.035} As _{0.965} + 100 nm GaAs
A2	1000 nm GaAs
B2	5 × (100 nm GaN _{0.035} As _{0.965} + 100 nm GaAs)

strain is intentionally brought into buffer structures on commercial substrates and relax majorly through the formation of cracks. Random rectangle-shaped surface patterns in micrometer range are successfully created by the formation of intersected crack networks by tensile strained InGaAs and InGaNs structures and have been shown to effectively relax the strain, examined both experimentally and by finite element method (FEM) analysis. The patterns formed in this work can work as virtual substrates for further growth of structures with lattice mismatch to the GaAs substrates. The strain will be mostly relaxed through elastic deformation leading to low threading dislocation density.

The samples were grown by molecular beam epitaxy (MBE) in an EPI930 (VEECO) system. First, a linearly graded In_xGa_{1-x}As ($x = 0.02-0.3$) layer is grown on GaAs substrate at 450 °C after the de-oxide of the substrate at 580 °C measured by a thermocouple. Second, a 500 nm In_{0.2}Ga_{0.8}As layer is grown at 500 °C, whose lattice constant is closely matched to the in-plane lattice constant of the partially relaxed top part¹⁵ of the graded buffer layer. Above this layer, four samples with different crack forming structures, which are summarized in Table I, are grown at 500 °C.

The surfaces morphology of the samples were characterized by atomic force microscopy (AFM). The structural properties were characterized by X-ray diffraction (XRD). The residual strain field in the samples after relaxation is simulated by FEM.

The sample A1 with 200 nm tensile strained GaAs as the crack forming layer was firstly grown and surface cracks successfully formed, as shown in Fig 1(a). The lattice mismatch between the GaAs and the In_{0.2}Ga_{0.8}As layer is about 1.4%. At the same time, another sample was designed and grown with a 200 nm In_{0.8}Ga_{0.2}As layer grown on top of an InAs buffer layer, which has the same 1.4% lattice mismatch. It was found that the tensile strain in the In_{0.8}Ga_{0.2}As layer was relaxed through surface roughening, instead of forming cracks, probably due the stiffness difference between In_{0.8}Ga_{0.2}As and GaAs, and will not be discussed further in this paper. From Fig. 1(a) we can see that, besides the line shaped cracks, oval shaped holes are another major feature. The formation of these holes would act similarly as surface roughening in the process of strain relaxation. In a larger view of AFM scan (not shown here), the distribution of the holes and cracks is not uniform, meaning for some regions it is mostly holes while for other regions majorly cracks. The cracks extend along the (110) and the (1-10) directions forming rectangular shaped patterns. Fig. 1(e) shows a 3-dimensional (3D) view of a zoomed in region with both cross-sectional cracks and holes. It can be seen that within the rectangular area surrounded by cracks, the surface is smooth while the edges warp up a bit due to the contraction after strain relaxation.

The formation of holes is not desired for the aim of natural patterning. Nitrogen was introduced to the next sample, B1, forming a GaNAs layer with the N concentration of 3.5%. The incorporation of N not only brings in more tensile strain but also increases the stiffness.^{12,16} Almost crack only morphology without any holes is observed on the sample B1 and Fig. 1(b) shows an AFM image of one typical region. The cracks distributes uniformly in both directions forming nice surface pattern. At some of the crossing points of the cracks, hole like features can be found but much smaller than those in the sample A1. Without the influence of the holes, other features, like the cross-hatch, is revealed. The cross-hatch pattern is typical for metamorphic growth, resulted from the misfit dislocations beneath,¹⁷ especially for the graded buffers. In the samples in this work, it is believed to come from the InGaAs graded buffer layer.

In order to see the evolution of the crack pattern with thickness another two samples A2 and B2 were grown. For A2, it is just that the thickness of the top GaAs layer is increased to 1 μm compared with A1, while for B2, it is a repeating structure of 100 nm GaAs and 100 nm GaNAs for five

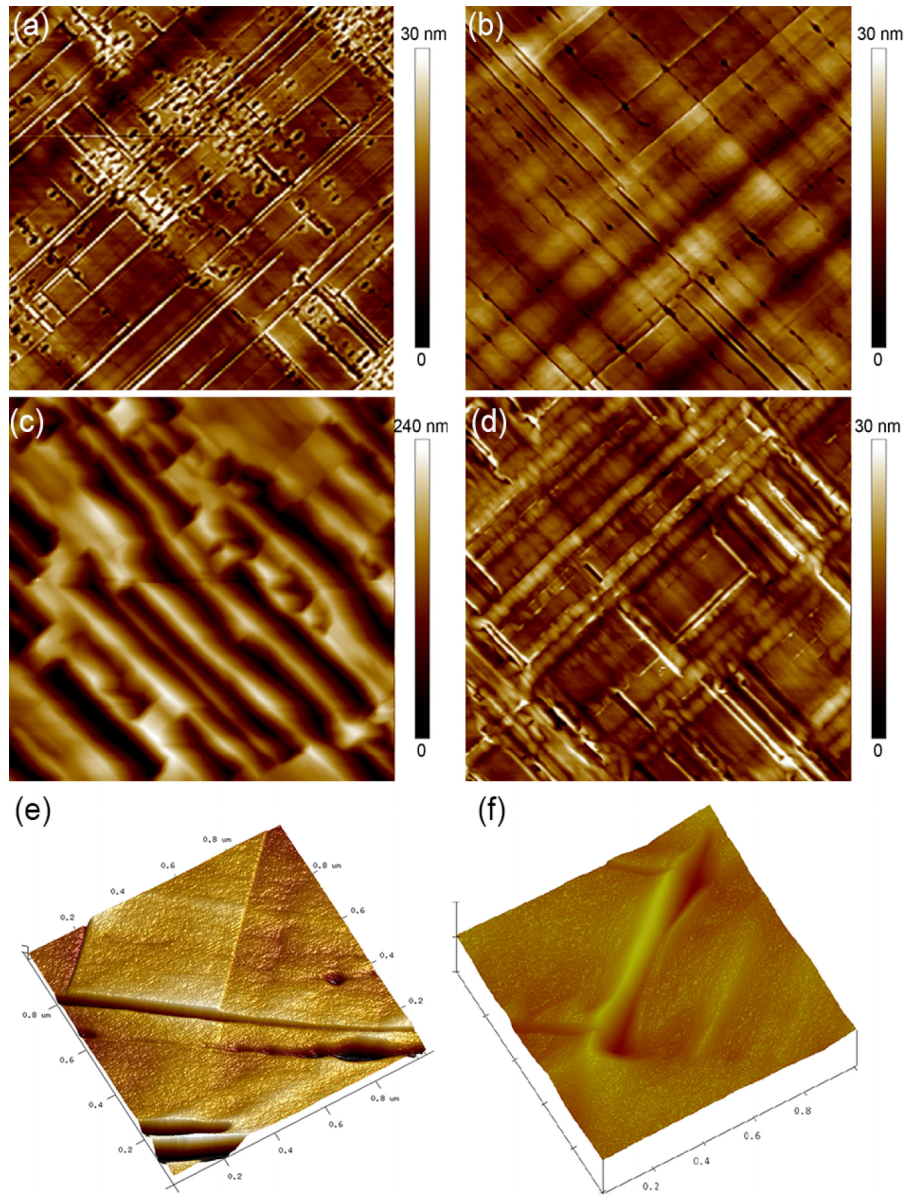


FIG. 1. AFM images of the samples. (a) - (d) are $10 \times 10 \mu\text{m}^2$ AFM images of the samples A1, A2, B1 and B2, respectively. (e) and (f) are $1 \times 1 \mu\text{m}^2$ 3D AFM images showing the cracks of the sample A1 and B2, respectively.

periods with the same total thickness as the sample A2. The situation is very different for these two samples as shown in Fig. 1(c) and 1(d). The surface of the sample A2 becomes very rough (RMS roughness= 46 nm) with deep grooves majorly along one of the $\langle 110 \rangle$ directions. However, the surface of B2 looks not very different from B1 although the cross-hatch pattern is more pronounced. A region with cracks is zoomed in and shown in 3D in Fig. 1(f). The deformation at the edges of the rectangular pattern is larger than that in the thinner sample of B1. The depth of the cracks cannot be accurately measured due to the size effect of the AFM tips.

Figure 2 shows the XRD rocking curves of the four samples. Among all of them, the tallest peak is from the GaAs substrates, an $\text{In}_{0.2}\text{Ga}_{0.8}\text{As}$ peak can be found at the small omega angle side (left side), and in between is a slope from the $\text{In}_x\text{Ga}_{1-x}\text{As}$ graded buffer layer. The layers with residual tensile strain can be seen at the right side of the GaAs substrate peak. In Fig. 2(a), a clear peak can be found with larger omega angle (right side) than the GaAs substrate peak, which is from

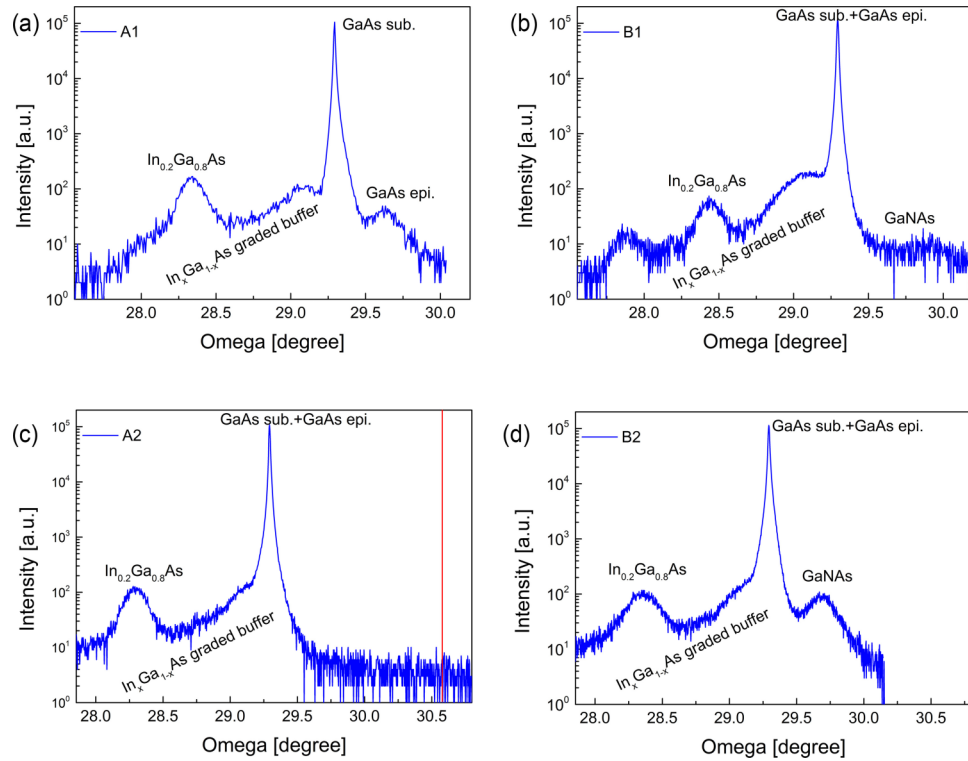


FIG. 2. XRD (115) rocking curves for the samples A1 (a), B1 (b), A2 (c) and B2 (d), respectively. The major peaks are labeled. The red line in (c) marks the peak position of the top GaAs layer if it is fully strained to the $\text{In}_{0.2}\text{Ga}_{0.8}\text{As}$ layer below.

the tensile strained top GaAs layer, whose in-plane lattice constant is smaller than the free GaAs. The existence of this peak demonstrates that the tensile strain in the 200 nm thick GaAs layer is partially relaxed but not complete. Based on four XRD (115) rocking curves with 0 and 180 degree rotation angles to eliminate the unintentional tilting, the relaxation rate is determined to be 93.8%. Similarly, the GaNAs in sample B1 shown in Fig. 2(b) is also partially relaxed. To the contrast, the peak of the top 1 μm GaAs layer is totally absent in Fig. 2(c). The red line marks the position if this layer is fully strained to the $\text{In}_{0.2}\text{Ga}_{0.8}\text{As}$ layer. For a partially relaxed tensile-strained GaAs layer, the peaks must lie between the GaAs substrate and red line. Therefore, the peak of the top GaAs layer must have coalesced with the GaAs substrate peak. A shoulder can be found at the right side of the GaAs substrate peak, which could be from the top GaAs layer, indicating an almost 100% strain relaxation. The signal of the GaNAs layers in the crack forming region in Fig. 2(d) is also found moved to the left compared with that in Fig. 2(b) showing larger strain relaxation of the GaNAs layer in the sample B2 than that in B1.

FEM analyses were carried out to simulate the strain field of the patterns formed by cracks. No strain relaxation through the formation of dislocations is assumed. A $1\ \mu\text{m} \times 1\ \mu\text{m} \times 100\ \text{nm}$ GaAs plate on an $\text{In}_{0.2}\text{Ga}_{0.8}\text{As}$ layer is built as a simplified model of the pattern on the sample A1. After relaxation, some of the strain components are shown in Fig. 3(a)-3(d). (a) is a 3D view of the ε_{xx} strain component at the surface of the rectangular pattern after strain relaxation. The deformation is also illustrated with a 14 times exaggeration. The simulated shape of the pattern meet well with the warping up shape in Fig. 1(e) and 1(f). Fig. 3(b) is an x - z plane slice of Fig. 3(a) from the center. From both Fig. 1(a) and 1(b) it can be found that the tensile strain at the four top corners relaxes most, which is in consistency with the fact that it also deforms most at the top corners. The center is mostly strained. The more inside the pattern, the less the strain is relaxed. Compressive strain is brought into the $\text{In}_{0.2}\text{Ga}_{0.8}\text{As}$ layer beneath the pattern, while around the corners tensile strain also appear in the $\text{In}_{0.2}\text{Ga}_{0.8}\text{As}$ layer. It is shown in Fig. 3(c) and 3(d) that shear strain components

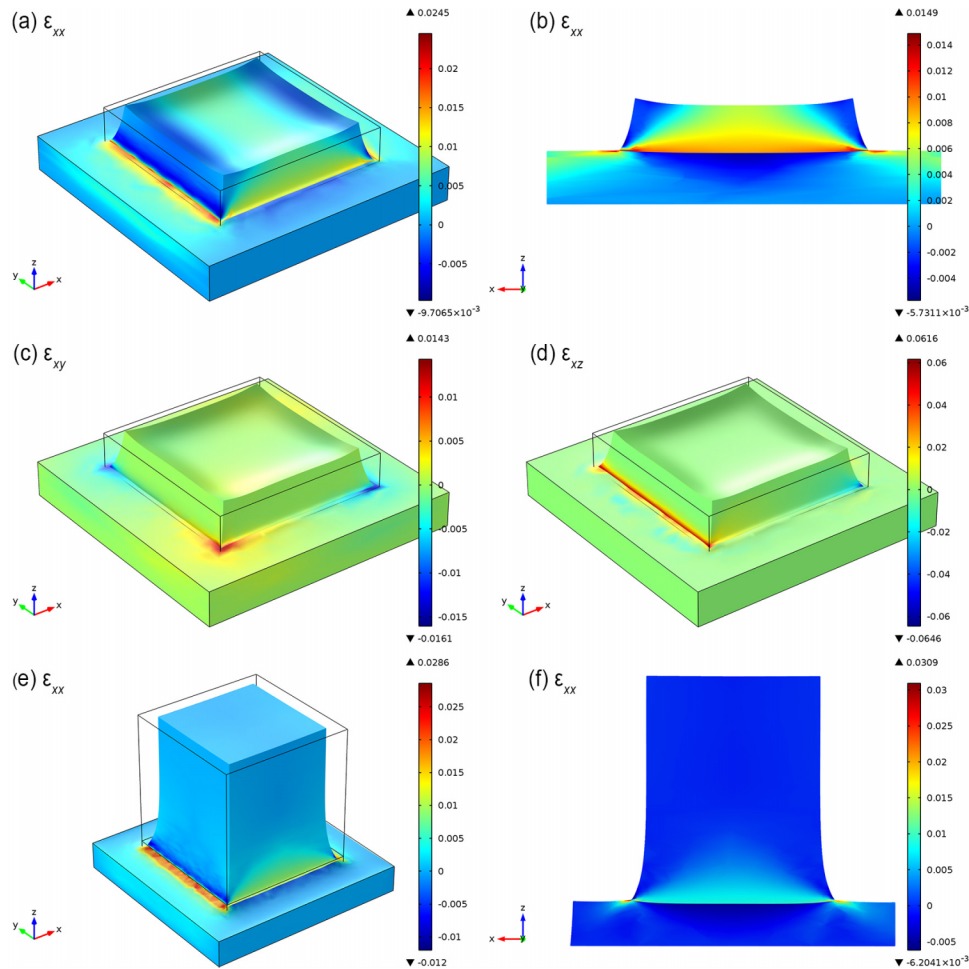


FIG. 3. Residual strain simulated by FEM. (a) - (d) simulates a pattern similar to the sample A1 with a $1 \mu\text{m} \times 1 \mu\text{m} \times 200 \text{ nm}$ GaAs pattern on $\text{In}_{0.2}\text{Ga}_{0.8}\text{As}$. (a), (c) and (d) are 3D views of the strain components ϵ_{xx} , ϵ_{xy} and ϵ_{xz} , respectively, and (b) is a x - z plane slice through the center showing ϵ_{xx} . (e) and (f) show the ϵ_{xx} distribution in the pattern when the thickness is increased to $1 \mu\text{m}$ (similar to the sample A2). (e) is a 3D view and (f) shows a slice through the center. Tensile strain is positive values. All the deformation is 14 times exaggerated.

arise after the strain relaxation with non-neglectable values. All the shear strain components has the largest values at the bottom corners or the bottom edges with values as large as 0.062 for the ϵ_{xz} .

Figure 3(e) and 3(f) show the simulation results when the pattern model in (a)-(d) increased to $1 \mu\text{m}$ thick, which can mimic the case of the sample A2. (e) is a 3D view of the ϵ_{xx} on the surface and (f) is an x - z plane slice of (e) from the center. The distribution of ϵ_{xx} is similar to that in (a) and (b) but fades to zero towards the top. It is shown that when the thickness reaches about 300 nm the tensile strain on the top can be almost fully relaxed purely through elastic deformation. This result is consistent with the XRD result shown in Fig. 2(c).

Comparing the sample A1 and A2, no cracks form when the top GaAs layer is 200 nm thick, while the morphology changes dramatically when it is $1 \mu\text{m}$ thick, as shown in Fig. 1(a) and 1(c). The origin of the grooves on sample A2 is not clear. It seems at least partly still related to the cracks beneath. Equivalently, the groove shape increases the surface area and relax the strain through roughening. During the epitaxy process between 200 nm and $1 \mu\text{m}$ thick, the tensile strain builds up more and more and finally the roughening mechanism seems to have won the competition with formation of cracks. For the sample B2, even more total tensile strain was accumulated but the surface morphology remain similar to the sample B1. We assume that the stiffness factor plays a dominant role. The GaNAs layers is harder than GaAs and can favor crack formation over surface roughening.

The ultimate aim to produce the surface pattern is to create devices/structures above the pattern with different lattice constants compared with the GaAs substrate and maintain low strain and low threading defects at the same time. From this work, the introduction of N significantly improve the morphology of the patterns formed by cracks. For the future work, layers with different lattice constants, e.g. InGaAs layers with large In composition, can be grown based on the structure of sample B2. Although lattice mismatch still exists between this layer and the GaAs/GaNAs pattern below, the finite size of the pattern will allow the strain to be relaxed majorly through elastic deformation¹⁸ and maintain high structural quality.

We have proposed and implemented the method of naturally forming surface patterns monolithically on GaAs substrates by the formation of cracks in tensile strained layers. With the help of N, the tensile strain relaxes purely by cracks instead of hole formation or surface roughening. The residual strain in the patterns is characterized experimentally and theoretically. For the samples with 1 μ m thick crack forming layers, the strain is found efficiently relaxed. The pattern created in this work can serve as templates to grow future structures, whose lattice constants are different compared with that of the commercial substrates, with low strain relaxation and few threading defects. Moreover, all the steps of this method is done in one growth run without pre-preparation nor re-growth and therefore is a convenient, clean and cost effectively approach.

ACKNOWLEDGEMENTS

The authors would like to thank the financial support from the Shanghai Pujiang Program (Grant No.14PJ1410600), the “Strategic Priority Research Program” of the Chinese Academy of Sciences (Grant No. XDA5-1), the Key Research Program of the Chinese Academy of Sciences (Grant No. KGZD-EW-804), and the Creative Research Group Project of Natural Science Foundation of China (Grant No. 61321492).

- ¹ Y. Song, S. Wang, I. Tangring, Z. Lai, and M. Sadeghi, *J. Appl. Phys.* **106**, 123531 (2009).
- ² I. Tangring, Y.X. Song, Z.H. Lai, S.M. Wang, and A. Larsson, *J. Cryst. Growth* **311**, 1684 (2009).
- ³ Y.B. Bolkhovityanov, A.S. Deryabin, A.K. Gutakovskii, M.A. Revenko, and L.V Sokolov, *J. Appl. Phys.* **96**, 7665 (2004).
- ⁴ B. Bertoli, D. Sidoti, S. Xhurxhi, T. Kujofsa, S. Cheruku, J.P. Correa, P.B. Rago, E.N. Suarez, F.C. Jain, and J.E. Ayers, *J. Appl. Phys.* **108**, 113525 (2010).
- ⁵ U.J. Lewark, A. Tessmann, A. Leuther, T. Zwick, O. Ambacher, and I. Kalfass, in *Microw. Integr. Circuits Conf. (EuMIC)*, (2013) 2013 Eur. 125.
- ⁶ M. Zaknoute, B. Bonte, C. Gaquiere, Y. Cordier, Y. Druelle, D. Theron, and Y. Crosnier, *Electron Device Lett. IEEE* **19**, 345 (1998).
- ⁷ I. Tangring, H.Q. Ni, B.P. Wu, D.H. Wu, Y.H. Xiong, S.S. Huang, Z.C. Niu, S.M. Wang, Z.H. Lai, and A. Larsson, *Appl. Phys. Lett.* **91**, 221101 (2007).
- ⁸ S.M. Wang, I. Tangring, Q.F. Gu, M. Sadeghi, A. Larsson, X.D. Wang, C.H. Ma, I.A. Buyanova, and W.M. Chen, *Thin Solid Films* **515**, 4348 (2007).
- ⁹ D. Wu, H. Wang, B. Wu, H. Ni, S. Huang, Y. Xiong, P. Wang, Q. Han, Z. Niu, I. Tangring, and S.M. Wang, *Electron. Lett.* **44**, 474 (2008).
- ¹⁰ Z. Mi, J. Yang, P. Bhattacharya, and D.L. Huffaker, *Electron. Lett.* **42**, 121 (2006).
- ¹¹ I.J. Fritz, P.L. Gourley, L.R. Dawson, and J.E. Schirber, *Appl. Phys. Lett.* **53**, 1098 (1988).
- ¹² Y. Song, S. Wang, Z. Lai, and M. Sadeghi, *Appl. Phys. Lett.* **97**, 91903 (2010).
- ¹³ Y. Song, S. Wang, X. Cao, Z. Lai, and M. Sadeghi, *J. Cryst. Growth* **323**, 21 (2011).
- ¹⁴ C. V Falub, H. von Känel, F. Isa, R. Bergamaschini, A. Marzegalli, D. Chrastina, G. Isella, E. Müller, P. Niedermann, and L. Miglio, *Science (80-.)* **335**, 1330 (2012).
- ¹⁵ J. Tersoff, *Appl. Phys. Lett.* **62**, 693 (1993).
- ¹⁶ J. Schone, E. Spiecker, F. Dimroth, A.W. Bett, and W. Jager, *Appl. Phys. Lett.* **92**, 81903 (2008).
- ¹⁷ Y.S. Sergey, J. Flemming, and P. Jon Wulff, *Appl. Phys. Lett.* **64**, 3305 (1994).
- ¹⁸ H. Ye, P. Lu, Z. Yu, Y. Song, D. Wang, and S. Wang, *Nano Lett.* **9**, 1921 (2009).